16th World Conference on Earthquake Engineering, 16WCEE 2017
Santiago Chile, January 9th to 13th 2017
Paper N° 2898
Registration Code: S-F1464334196

EMPIRICAL DYNAMIC AMPLIFICATION FACTORS FOR SITES BASED ON SEISMIC NOISE

B. Idini[(1)], F. Rojas[(2)], N. Ruiz[(3)], C. Pastén[(4)], F. Leyton[(5)]

[(1)] *Graduate Researcher, Departmet of Civil Engineering, University of Chile, Santiago, Chile, e-mail: bidini@ing.uchile.cl*
[(2)] *Assistant Profesor, Departmet of Civil Engineering, University of Chile, Santiago, Chile, e-mail: frojas@ing.uchile.cl*
[(3)] *Assistant Profesor, Departmet of Geophysics, University of Chile, Santiago, Chile, e-mail: sruiz@dgf.uchile.cl*
[(4)] *Assistant Profesor, Departmet of Civil Engineering, University of Chile, Santiago, Chile, e-mail: cpasten@ing.uchile.cl*
[(5)] *Senior Seismologist, National Seismological Center, University of Chile, Santiago, Chile, e-mail: leyton@csn.uchile.cl*

Abstract

Seismic demand determination for structures and quantification of seismic hazard of a region require the evaluation of the local site effects, such as the dynamic amplification of the soil. Commonly, there are two parameters that the most modern models and seismic codes use independently to quantify this phenomenon. One is the fundamental period of the soil or To (Japanese code) and the second is the average shear wave velocity up to 30 m depth or V_{S30} (North American and European codes). However, none of these two parameters has managed to explain acceleration records in large Chilean earthquakes, such as the records in the Concepción city during the 2010 Mw 8.8 Maule Earthquake. In this paper, an empirical model to quantify the dynamic amplification of soil at periods from 0.01 s to 10 s, using the 5% damped H/V response spectral ratios (HVRSR) obtained from earthquake acceleration records at seismic stations located in Chile, is developed. The amplification factor is expressed in terms of the soil predominant period (T*) and the peak value of the average HVRSR of the site. The predominant soil period allows to describe the spectral shape factor, while the peak value of the HVRSR determines its amplitude, which make the proposed model unprecedented. The results can be used to assess the seismic hazard in a variety of sites and to derive ground motion prediction equations for the Chilean region or other region with similar seismological and geological characteristics. In addition, the results could allow projecting future changes in the determination of the seismic demand on the official Chilean Earthquake Resistant Design code (NCh433).

Keywords: dynamic amplification, site effects, ground motion.

1. Introduction

Site effects are a crucial aspect in the seismic demand estimation of earthquake resistant design codes, in seismic hazard studies for structures, and in the derivation of ground motion prediction equations. It can be defined using two different relationships. The first definition is the ratio between the surface response to an earthquake and the rock basement response. The second definition is the ratio between the surface response to an earthquake and the outcrop response. Usually the second definition is more frequently used in seismic design due to the possibility of measuring the site response directly at the surface.

The methodologies to measure the site effects are diverse. [1] use the Fourier amplitude spectra (FAS) of strong motion records of the same earthquake at a reference outcrop site and at a near soil site to determine the empirical transfer function between them. [2] use a similar methodology than [1] but they use the 5%-damped response spectra of the strong motion records. [3] develop a technique to approximate empirical transfer function of the soil respect to basement from the horizontal-to-vertical FAS ratio of microtremors measures at the soil site.

In addition, considering the practical use, seismic codes try to account for site effects in a simplified way by using parameters that can be easily measured from the site. The two most common parameters are the predominant period of the soil T* (Japanese code) and the shear wave velocity up to 30 m depth V_{S30} (US and Europe codes).

In this paper we use a variation of the Nakamura's principle [3] applied to the horizontal-to-vertical ratios of the 5%-damped response spectra of strong motion records (HVRSR) to account for the site effects in Chilean seismic stations sites. Following the approach of [4, 5, 6], we classify the sites with a criterion based on the predominant period identified from the average HVRSR of every site. Finally, we derive an empirical model for the site effects coefficients as function of T* and the peak value of the HVSR derived from the Nakamura's technique that can be used in strong motion models and seismic hazard studies. The Nakamura's technique uses records of seismic noise obtained at a given site to account for amplification effects [3]. As the records are obtained at the surface, this technique does not requires drilling a borehole at the site.

2. Database

The strong motion database used was selected from the compilation of Chilean earthquake records described in [7]. All the 1115 records, which have a source-to-site distance as close as 400 km were used, are from 184 interface and intraplate Mw >= 5.5 earthquakes. The processing of the data was performed using the [8, 9] considerations, which leads to average HVRSRs with different available longest period depending on the station and the characteristics of their instrument (Fig. 1). A deep characterization of the ground motion levels of the database can be found in [10].

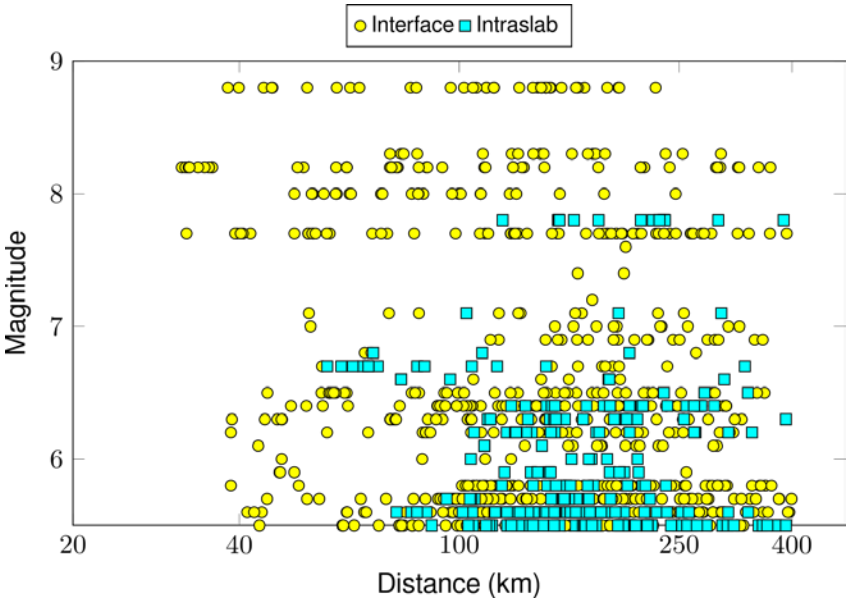

Fig. 1 – Chilean database used in this study [7].

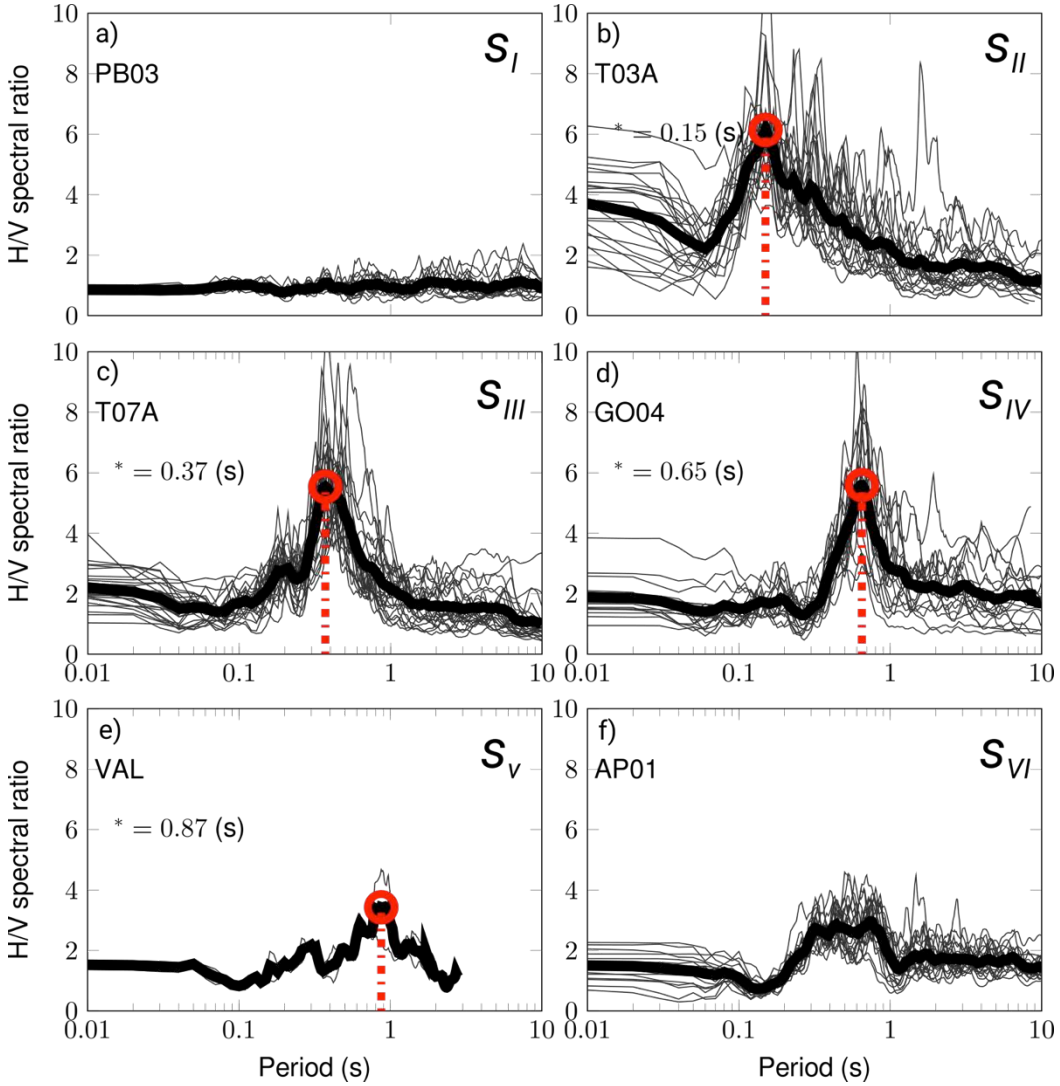

Fig. 2 – Examples of seismic stations site classification using the Table 1.

Table 1 – Predominant period T^* site classification.

Site class	T^* (s)	# Stations
s_I	Not identifiable: HVRSR <= 2	35
s_{II}	T^* <= 0.2	15
s_{III}	0.2 < T^* <= 0.4	33
s_{IV}	0.4 < T^* <= 0.8	28
s_V	T^* > 0.8	11
s_{VI}	Not identifiable: broad band amplification or 2+ peaks	32

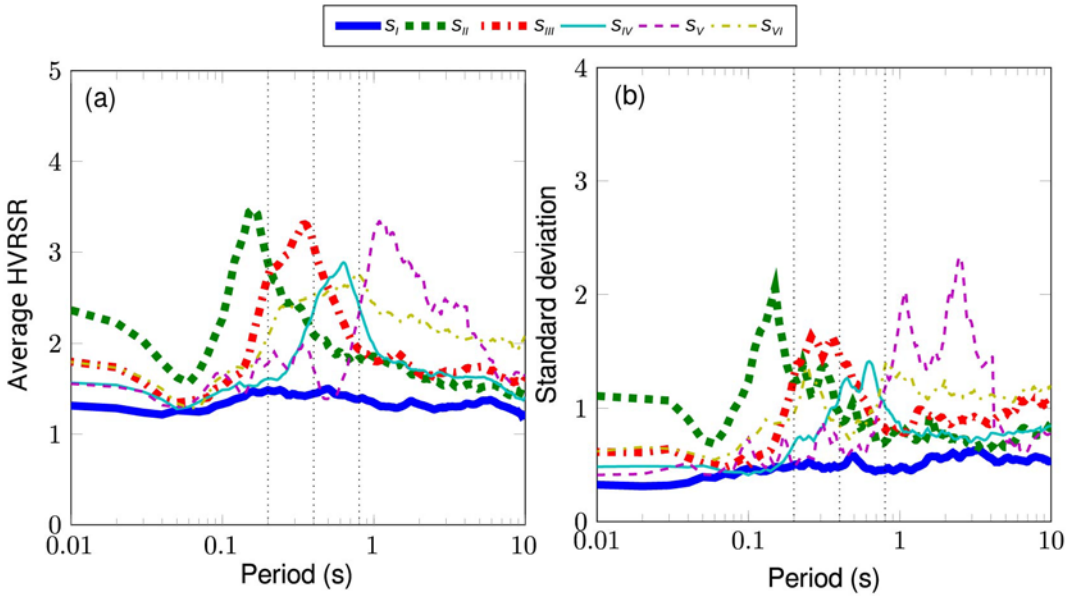

Fig. 3 – (a) Average HVRSRs and (b) standard deviations of the soil site classification described in Table 1.

3. Soil Classification

We define the predominant period of a station T* as the period at which the average HVRSR peaks P* [4, 5, 6]. If the average HVRSR does not show a pronounced peak, as Fig. 2a shows for the PB03 site, the station is identified as reference rock site s_I. If the average HVRSR has multiple peaks or broadband amplification, as Fig. 2f shows for the AP01 site, the station is identified as generic soil s_{VI}. Soil sites s_{II}, s_{III}, s_{IV}, and s_V depend on T* according to Table 1. Fig. 2 shows the classification of the T03A, T07A, and GO04 sites, which are examples of stations with a clear HVRSR peak (T*, P*). We classified 135 seismic station sites using the 1207 available strong motion records of interface and intraslab earthquakes, the complete Chilean earthquake database used in this study [7]. Fig. 3a and Fig. 3b show the average HVRSR and the standard deviation of all the seismic stations classified with the predominant period criteria from s_I to s_{VI}. The soil site classification as a function of T* in Fig. 3a shows that the average spectra of each of the six site classes have relativity similar shape and amplitude, except for the reference rock site s_I and the generic soil s_{VI}. However, Fig. 3b shows that the peak standard deviation, associated to the average HVRSR presented in Fig3a, is reached near P* for every site class.

4. Empirical Site Effects Coefficients

Using the classification described before, the strong motion spectra produced by an earthquake can be conveniently decoupled as the contributions of the seismic source F, the trajectory to the site D, and the local site effects f_s [10]:

$$S_{hs}(T) = S_{hr}(F,D) f_s(T) \quad (1)$$

where S_{hs} is the horizontal response spectra at a given soil site condition, S_{hr} is the horizontal response spectra at a rock site as function of F and D, and f_s is a spectral shape factor that describes the modification of the rock site response spectra by the local site conditions.

We assume that the shape factor $f_s(sta)$ at the seismic station can be obtained from the average H/V response spectral ratio (HVRSR), normalized by the average HVRSR at a reference rock site [6].

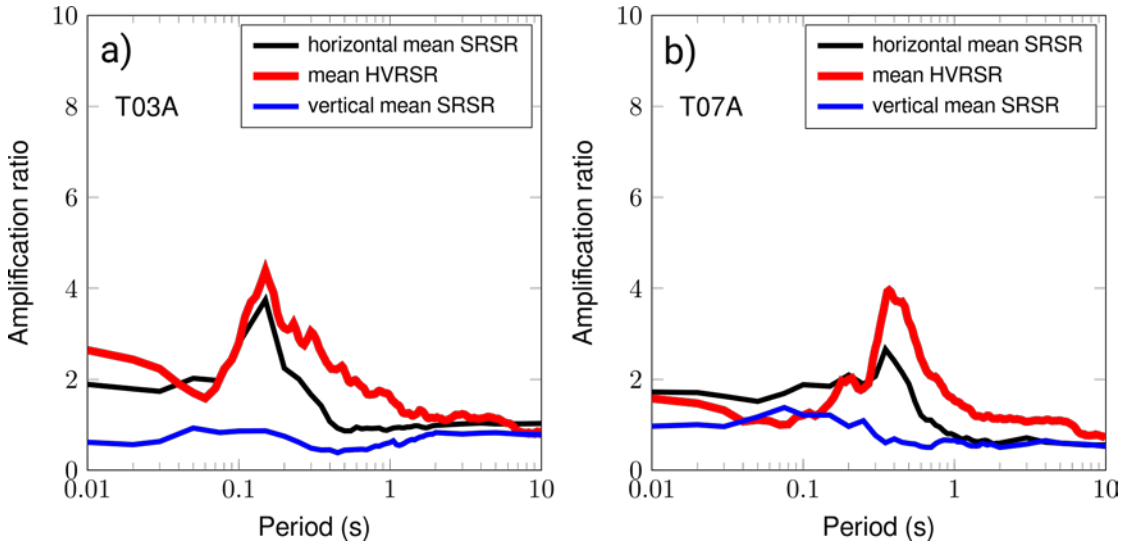

Fig. 4 – Comparison of the amplification ratio accounted by the average HVRSR and the average SRSR at (a) T03A station and (b) the T07A station.

The f_s factor of a seismic station site is defined as:

$$f_s(sta)(T) = \frac{HVRSR_{(sta)}}{HVRSR_{(I)}} = \frac{\frac{S_{hs}}{S_{vs}}}{\frac{S_{hr}}{S_{vr}}}(T) \quad (2)$$

where $HVRSR_{(sta)}$ is the average HVRSR at the seismic station, $HVRSR_{(I)}$ is the average HVRSR of the reference rock sites s_I, S_{vs} is the vertical response spectra at a given soil site condition, and S_{vr} is the vertical response spectra at a rock site. Hence, Eq. (1) can be written as:

$$S_{hs}(T) = S_{hr} \frac{\frac{S_{hs}}{S_{vs}}}{\frac{S_{hr}}{S_{vr}}}(T) = S_{vr} \frac{S_{hs}}{S_{vs}}(T) \quad (3)$$

Assuming that the vertical component of the ground motion at the soil site does not amplify with respect to the vertical component in the rock site ($S_{vr} = S_{vs}$), the use of $f_s(sta) = HVRSR_{(sta)}/HVRSR_{(I)}$ is justified. It is worth noting that $HVRSR_{(I)}$ is approximately 1.4 along all the studied period domain. Fig. 4 shows validation examples of the method considering the Iquique City seismic stations T03A and T07A. The site response spectral ratio (SRSR) in Fig. 4 represent the average ratio between response spectra of the respective seismic station over the response spectra of a near rock reference site (T04A in both cases of Fig. 4) computed for a set

of common earthquakes with available strong motion records. The flat shape of the vertical average SRSR in both seismic stations of Fig. 4 shows that there is no amplification in the vertical component. The amplification accounted by the average HVRSR is highly similar to those accounted for horizontal average SRSR.

The classification in Table 1 leads to f_s coefficients with high variability in amplitude, as Fig. 3b shows. To account for this variability, we adopted an additional parameter to derive f_s based on the contrast between the maximum amplitude of the average f_s for a seismic station and the maximum amplitude of the average f_s of their site class. Fig. 5 shows the average f_s factors for different seismic stations compared to the average f_s of their respective k soil site class (k = II, III, IV, or V). For each soil site s_k in Fig. 5, the thick solid line represents the average f_s factor for the class s_k and the thin solid line the average f_s factor for a seismic station that was classified with the same soil site. For any seismic station with soil site s_k, their f_s factor can be written in terms of the average f_s factor of the soil site s_k and a parameter *n*, as follows:

$$f_s(sta) = [f_s(s_k)]^n \tag{4}$$

where *n* is defined as:

$$n = \frac{\log_{10}[f_s^*(sta)]}{\log_{10}[f_s^*(s_k)]} \tag{5}$$

and f_s^* is the peak value of the average f_s. Hence, the f_s factor in Eq. (2) can be represented by the average f_s as:

$$f_s(T) = \left(\frac{HVRSR_{(k)}}{HVRSR_{(I)}}\right) \tag{6}$$

where $HVRSR_{(k)}$ is the average HVRSR of the soil site s_k or that of the generic soil site s_{VI}. For the reference rock sites s_I, we assume that there is no dynamic amplification and s(T*) = 1. Soil sites with non-identifiable predominant period or broad band amplification, are considered as generic soil s_{VI}. For generic soil s_{VI} and those with identifiable predominant period soils, their s(T*) values are presented in Table 2 and should be used following the predominant period site classification described in Table 1.

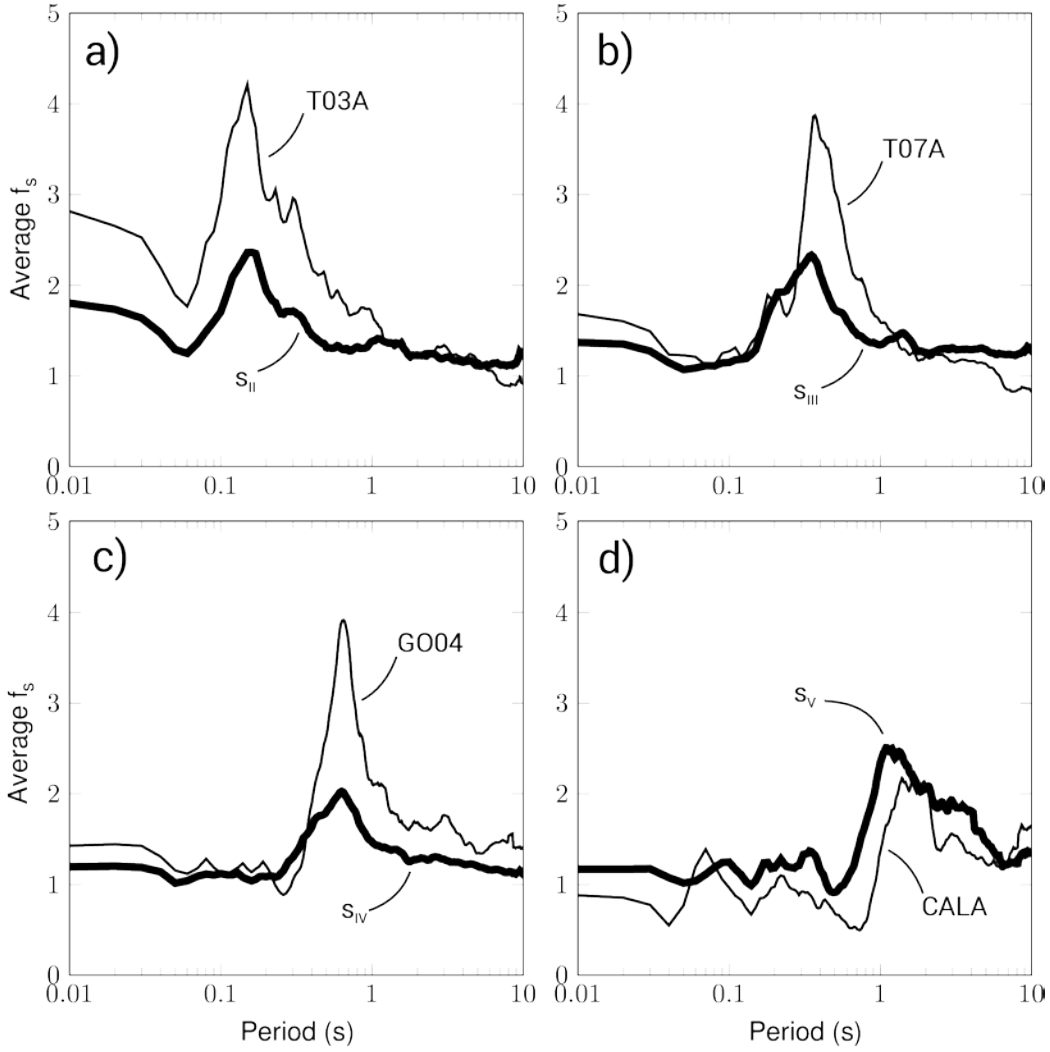

Fig. 5 – Site effect coefficient average f_s computed for seismic stations (a) T03A, (b) T07A, (c) GO04, and (d) CALA, compared with their respective soil sites s_{II}, s_{III}, s_{IV}, and s_V.

4.1 Empirical amplification factors from seismic noise

The required acceleration earthquake records needed to compute the average HVRSR are not always available. An approximation to the T* of a soil site can be obtained from the H/V spectral ratio (HVSR) computed using seismic noise time series and the Nakamura's technique [3].

The n parameter defined in Eq. (5) can be also obtained using the Nakamura's technique. Fig. 6 shows the HVSR peak value (N*) computed by Leyton [11] for a subset of Chilean seismic stations versus the peak value of the f_s factor, which was defined in Eq. (2) and computed in this study. A least squares regression was performed between both parameters using the relation:

$$f_s^*(sta) = b \log_{10}(N^*) + a \quad (7)$$

The regression was constrained to a = 0 and the results were b = 6.04 with R = 0.92 and, $\sigma = 1.15$. The standard deviation was computed from the difference between the $f_s^*(s_k)$ data values and their predictions evaluated with Eq. (7). Fig. 6 shows the evaluation of these results in a thick solid line. Non-linear effects are not considered in this study and the relation might not be consistent for N* > 7.

To account for a unique value of $f_s^*(s_k)$ in Eq. (5), we computed the weighted average of the peak values of the average f_s factors shown in Fig. 5 (thick lines), with weights equal to the number of records in every soil site class s_k. Hence, the *n* parameter in Eq. (4) can be empirically determined as function of the peak value of the HVSR (N*) using the Nakamura technique and the empirical relation:

$$n = 2.82 \log[\log(N^*)] + 2.20 \tag{8}$$

For a more conservative dynamic analysis, Fig. 6 also shows an envelope regression (R = 0.99, $\sigma = 0.39$) that considers the stations with the greatest f_s^* values. In this case, the empirical relation between n and N* is given by:

$$n = 2.82 \log[\log(N^*)] + 2.56 \tag{9}$$

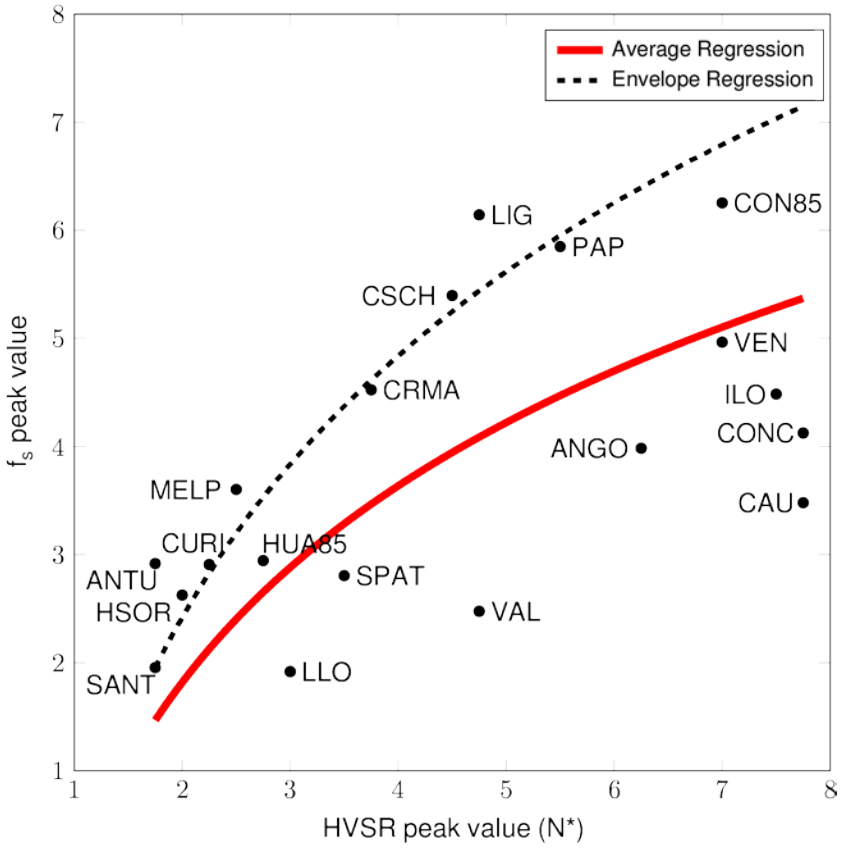

Fig. 6 – Regression model between peak H/V Nakamura values and peak values of the average HVRSRs for different seismic stations.

Table 2 – Site effect coefficients $f_s(s_k)$ for different soil sites s_k.

Period (s)	s_{II}	s_{III}	s_{IV}	s_V	s_{VI}
PGA	1.878	1.415	1.126	1.096	1.256
0.01	1.756	1.326	1.115	1.091	1.231
0.02	1.638	1.251	1.106	1.088	1.210
0.03	1.522	1.188	1.098	1.086	1.193
0.05	1.389	1.010	1.086	1.086	1.171
0.07	1.459	1.062	1.080	1.092	1.164
0.10	1.757	1.098	1.081	1.111	1.183
0.15	2.105	1.436	1.110	1.178	1.301
0.20	2.058	1.801	1.149	1.236	1.472
0.25	1.874	2.064	1.214	1.270	1.613
0.30	1.724	2.193	1.323	1.270	1.696
0.40	1.514	2.167	1.581	1.176	1.779
0.50	1.381	1.981	1.787	1.110	1.822
0.75	1.345	1.530	1.862	1.451	1.905
1.00	1.345	1.315	1.647	2.033	1.875
1.50	1.307	1.293	1.376	2.377	1.755
2.00	1.264	1.283	1.261	2.247	1.675
3.00	1.213	1.266	1.250	1.971	1.642
4.00	1.202	1.265	1.255	1.77	1.620
5.00	1.199	1.265	1.244	1.600	1.604
7.50	1.199	1.265	1.180	1.316	1.598
10.00	1.199	1.265	1.143	1.283	1.598

5. Conclusions

Using strong motion data from interface and intraplate earthquakes with magnitudes Mw = 5.5 – 8.8 and distance limit of 400 km, an empirical site effect model to account for the soil amplification in the seismic demand estimation of earthquake design codes, seismic hazard analysis, and GMPE derivation based on seismic noise, is developed. The soil amplification factor is expressed in terms of the soil predominant period (T*), and the peak value of the average HVRSR of the site. The soil amplification factor is defined for 5 different types of soils, depending of the range of their predominant period. The predominant period allows localizing the period range of the response spectra where the amplification takes place. In addition, it is introduced a relationship

between the peak value of the average HVRSR of the site and the HVSR peak value (N*), due to the HVSR peak value can be empirically determined at any site using the Nakamura's technique [3], which simplify the use of this methodology.

To obtain the site effects coefficients for a given site, the user should evaluate Eq. (4) using the predominant period of the soil (T*) and the HVSR peak value of the site (N*). The predominant period of the soil should be used to classify the soil and select their $f_s(s_k)$ coefficients from Table 2. The HVSR peak value of the site should be used to evaluate n from Eq. (8) or Eq. (9) depending on the user's preferences.

6. Acknowledgements

This study was partially financially supported by Chile's National Commission on Scientific and Technological Research (CONICYT) for the Fondecyt Initiation into Research 2014 projects, National Research Funding Competition under Grant No. 11140429 and No. 11130230., and by CONICYT-PCHA/MagísterNacional/2014-22140466.

7. References

[1] Lermo J, Chávez-García FJ (1994): Site effect evaluation at Mexico City: dominant period and relative amplification from strong motion and microtremor records. *Soil Dyn Earthq Eng*, **13**(6), 413-423.

[2] Seed HB, Romo MP, Sun JI, Jaime A, and Lysmer J (1988): The Mexico Earthquake of September 19, 1985-Relationships Between Soil Conditions and Earthquake Ground Motions. *Earthq Spec*, **4**(4), 687-729.

[3] Nakamura, Y (1989): A method for dynamic characteristics estimation of subsurface using microtremor on the ground surface. *Railway Technical Research Institute, Quarterly Reports*, **30** (1).

[4] Zhao JX, Irikura K, Zhang J, Fukushima Y, Somerville PG, Asano A, Ohno Y, Oouchi T, Takahashi T, Ogawa H (2006a): An Empirical Site-Classification Method for Strong-Motion Stations in Japan Using H/V Response Spectral Ratio. *B Seismol Soc Am*, **96** (3), 914-925.

[5] Fukushima Y, Bonilla LF, Scotti O, Douglas J (2007): Site classification using horizontal-to-vertical response spectral ratios and its impact when deriving empirical ground-motion prediction equations. *J Earthq Eng*, **11**, (5), 712-724.

[6] Di Alessandro C, Bonilla LF, Boore DM, Rovelli A, Scotti O (2012a): Predominant-Period Site Classification for Response Spectra Prediction Equations in Italy. *B Seismol Soc Am*, **102** (2), 680-695.

[7] Idini B, Rojas F, Ruiz S, Pastén C (2016): Ground motion prediction equations for the Chilean subduction zone. Submitted to *Bulletin of Earthquake Engineering*.

[8] Boore DM, Boomer JJ (2005): Processing of strong-motion accelerograms: needs, options and consequences. *Soil Dyn Earthq Eng*, **25** (2), 93-115.

[9] Douglas J, Boore DM (2011): High-frequency filtering of strong-motion records. *B Earthq Eng*, **9** (2), 395-409.

[10] Idini B (2016): Curvas de atenuación para terremotos intraplaca e interplaca en la zona de subducción chilena, Graduate Degree Dissertation, Civil Engineering Department, University of Chile, 193 pp. (in Spanish).

[11] Boore DM, Atkinson GM (2008): Ground-motion prediction equations for the average horizontal component of PGA, PGV, and 5%-damped PSA at spectral periods between 0.01 and 10.0 s. *Earthq Spec*, **24**(1), 99-138.

[12] Leyton F: Personal Communication.